International Journal of Current Engineering and Technology
ISSN 2277 - 4106

Available at http://inpressco.com/category/ijcet

Research Article

Multi-Objective Optimization of Design Parameters of a Shell &Tube type Heat Exchanger using Genetic Algorithm

Sampreeti Jena[a], Pandaba Patro[b] and Siddhartha Shankar Behera[c]

[a]University of Minnesota, Twin Cities-55455
[b]Indian Institute of Technology, Kharagpur-721302
[c]National Institute of Technology, Rourkela-769008

Accepted 26 August 2013, Available online 01 October 2013, **Vol.3, No.4 (October 2013)**

Abstract

While there has been ample research on the optimization of heat exchangers from economic point of view using a wide range of algorithms, there has been no work to achieve the simultaneous optimization of 2 objectives- the annual sum of capital investment and working cost as well as the length of the heat exchanger. The given work has drawn a co-relation between the minimization of length and the minimization of length. We have clearly outlined the impact of minimization of one objective on the other. In order to achieve this we have implemented the multi-objective solver that uses genetic algorithm (gamultobj), available in the MATLAB optimization tool-box. The multi-objective algorithm(Elitist Multi-objective Genetic Algorithm) searches for the optimal values of design variables such as outer tube diameter, outer shell diameter and baffle spacing, for two types of tube layout arrangement (triangular and square) with the number of tube passes being two or four.

Keywords*: Heat, Exchanger, Cost, Optimization, Genetic*

1. Introduction

A shell-and-tube heat exchanger is a reincarnation of the double-pipe configuration. Instead of a single pipe within a larger pipe, it comprises of a bunch of pipes or tubes encased within a cylindrical shell. One fluid flows through the tubes, and a second fluid flows within the space between the tubes and the shell. Baffles are installed along the tube bundle to direct the fluid between the tubes and shell, across the tubes. Heat is exchanged between the fluids through the tube walls. The fluids can be either liquids or gases on either the shell or the tube side.

Most researchers consider the sum of capital investment and energy related costs associated with overcoming friction losses. Similarly, some authors may consider only pumping costs like Mott*et al*, 1972 or capital investment like Ramanand*aet al*, 1991) while others choose entropy generation or the ratio of performances to cost (Kovarik, 1989). Moving on to the optimization variables, most works aim for the simultaneous impact of several design parameters, while others may concentrate on a single parameter. For instance, Saffar-Avval and Damangir (1995) conducted studies for optimizing only the baffle spacing. Yet, parametric analysis methods were also implemented by Jenssen 1969, to examine the effects of multiple parameters. In numerical optimization methods, Lagrange multipliers were frequently (Kovarik 1989; Fax and Mills, 1957; Unuvar and Kargici, 2004). Fon-tein and Wassink (1978) used the simplex method, while Palen et al. (1974) utilized the so-called Complex method. Geometric programming was also proposed by Paul (1982) and in recent times, techniques such as, Simulated annealing including vibration constraints by Chauduri et al. (1997) and Geometric Algorithm by Selbas, Kizilkan and Reppich (2006)have been shown to be an effective approaches.

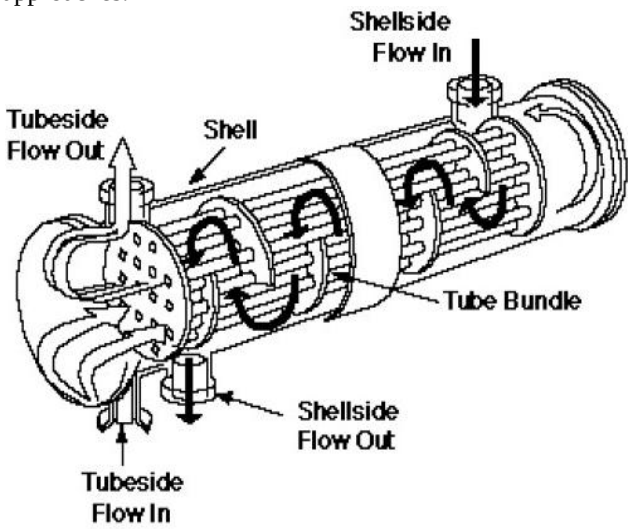

Figure 1: Tube and Shell side Flow

*Corresponding author: **Sampreeti Jena**

There has been no work, whatsoever, which aims to optimize the heat exchanger design variables while keeping an eye on its length. To find a solution of the optimized heat exchanger design problem, in this paper, a methodological approach aiming at the simultaneous minimization of total heat exchange-related costs and the length (physical dimension) is proposed deploying evolutionary computation techniques based on GA. The proposed method, starting from the user defined specifications, enables the direct definition of the heat exchanger configuration and dimensions by iteratively computing the values of the optimal design parameters that are able to satisfy the specification at the minimum total discounted cost and heat exchanger length. After briefly describing the design procedure as well as the choice of optimization variables, proper cost and length functions are selected and the optimization algorithm is performed.

2. Methodology

The optimization procedure was implemented by a multi-objective genetic algorithm (GA).Starting from an initial population of randomly created individuals representing candidate solutions, in this scenario, a heat exchanger of specific configuration and conforming to the design specifications, the GA uses the concept of survival of the fittest to produce more desirable individuals in subsequent evolutionary generations of the population. The cost value of each candidate solution denotes the fitness function of the individual which is a measure of its quality relative to the entire population.

The evolution starts from a population of randomly generated individuals and is an iterative process, with a new population in each iteration, called a generation. In each generation, the fitness of every individual in the population is computed; the fitness being the value of the objective function. The more fit individuals are stochastically elected from the current population, and each individual's genome is modified (recombined and possibly randomly mutated) to advance to a new generation. The new generation of candidate solutions is then utilized in the next iteration of the algorithm. Commonly, the algorithm terminates when either a maximum number of generations has been produced, or a satisfactory fitness level has been reached for the population.

The multi-objective genetic algorithm (gamultiobj) works on a population by using a set of operators that can be applied to the population. The initial population is generated randomly by default. The next generation of the population is derived from the non-dominated rank, which assigned to each individual using the relative fitness, and a distance measure of the individuals in the current generation.

Individual 'p' dominates 'q' ('p' has a lower rank than 'q') if 'p' is strictly better than 'q' in at least one objective and 'p' is no worse than 'q' in all objectives. This is same as saying 'q' is dominated by 'p' or 'p' is non-inferior to 'q'. Two individuals 'p' and 'q' are considered to have identical ranks if neither dominates the other. The distance measure of an individual is used to compare between individuals having the same rank by estimating how far an individual is from the other individuals with the same rank.

The multi-objective GA function "gamultiobj" uses a controlled elitist genetic algorithm (a variant of NSGA-II). While the elitist GA always favors individuals with better fitness value (lower rank), the controlled elitist GA also favors individuals that tend to increase the diversity of the population even if they have a lower fitness value. In order to ensure the convergence to an optimal Pareto front, it is very important to maintain the diversity of population. This is done by controlling the elite members of the population as the algorithm progresses, by using the options, 'ParetoFraction' and 'DistanceFcn'. The Pareto fraction option limits the number of individuals on the Pareto front (elite members) and the distance function helps to maintain diversity on a front by favoring individuals that are relatively far away on the front**.**

3. Governing equations

Mean logarithm temperature difference:

$$S = \frac{Q}{U\Delta T_{ML}F}, \quad (1)$$

F being the temperature difference corrective.

The heat transfer coefficient is computed through the following equations:

$$U = \frac{1}{\frac{1}{h_s}+R_{foul,shell}+\frac{d_o}{d_i}.(R_{foul,tube}+\frac{1}{h_t})} \quad (2)$$

$$d_i = 0.8d_o. \quad (3)$$

The tube-side heat transfer coefficient h_t is computed, according to the flow regime, resorting to the following correlations:

$$h_t = 0.027\frac{k_t}{d_o}Re_t^{0.8}.Pr_t^{1/3}\left(\frac{\mu_t}{\mu_{wt}}\right)^{0.14} \quad (4)$$

$(\text{for } Re_t > 10{,}000)$

Where, f_t is the Darcy friction factor given as,

$$f_t = (1.82\log 10^{Re_t} - 1.64)^{-2} \quad (5)$$

Re_t is the tube side Reynolds number and given by,

$$Re_t = \frac{\rho_t v_t d_i}{\mu_t} \quad (6)$$

Flow velocity for tube side is found by,

$$v_t = \frac{m_t}{(\pi/4)d_t^2\rho_t}\left(\frac{n}{N_t}\right) \quad (7)$$

N_t is the number of tubes and n is the number of tube passes which can be found approximately from the following equation,

$$N_t = C\left(\frac{D_s}{d_o}\right)^{n_1} \quad (8)$$

C and n_1 are coefficients that are taking values according to flow arrangement and number of passes. These coefficients are shown in Table 1 for different flow arrangements.

Pr_t is the tube side Prandtl number and given by,

$$Pr_t = \frac{\mu_t C_{pt}}{k_t} \quad (9)$$

Also, $d_i = 0.8 d_o$ (10)

Kern's formulation for segmental baffle shell-and-tube exchanger is used for computing shell side heat transfer coefficient h_s,

$$h_s = 0.36 \frac{k_t}{d_e} Re_s^{0.55} . Pr_s^{1/3} \left(\frac{\mu_s}{\mu_{wts}}\right)^{0.14} \quad (11)$$

Where, d_e is the shell hydraulic diameter and computed as,

$$d_e = \frac{4\left(S_t^2 - \left(\frac{\pi d_o^2}{4}\right)\right)}{\pi d_o} \text{(for square pitch)} \quad (12)$$

$$d_e = \frac{4\left(0.43 S_t^2 - \left(\frac{0.5\pi d_o^2}{4}\right)\right)}{0.5\pi d_o} \text{ (for triangular pitch)} \quad (13)$$

Cross Section area normal to flow direction is determined by, $A_s = D_s B \left(1 - \frac{d_o}{S_t}\right)$ (14)

$$v_s = \frac{m_s}{\rho_s A_s} \quad (15)$$

Reynolds number for shell side follows,

$$Re_s = \frac{m_s d_e}{A_s \mu_s} \quad (16)$$

Prandtl number for shell side follows,

$$Pr_s = \frac{\mu_s C_{ps}}{k_s} \quad (17)$$

The overall heat transfer coefficient (U) depends on both the tube side and shell side heat transfer coefficients and fouling resistances are given by,

$$U = \frac{1}{(1/h_s) + R_{fs} + (d_o/d_i)(R_{ft} + (1/h_t))} \quad (18)$$

Considering the cross flow between adjacent baffle, the logarithmic mean temperature difference (LMTD) is determined by,

$$LMTD = \frac{(T_{hi} - T_{co}) - (T_{ho} - T_{ci})}{\ln((T_{hi} - T_{co})/(T_{ho} - T_{ci}))} \quad (19)$$

The correction factor F for the flow configuration involved is found as a function of dimensionless temperature ratio for most flow configuration of interest.

$$F = \sqrt{\frac{R^2+1}{R-1}} \frac{\ln((1-P)/(1-PR))}{\ln((2-PR+1-\sqrt{R^2+1})/(2-PR+1+\sqrt{R^2+1}))} \quad (20)$$

Where R is the correction coefficient given by,

$$R = (T_{hi} - T_{ho})/(T_{co} - T_{ci}) \quad (21)$$

P is the efficiency given by,

$$P = (T_{co} - T_{ci})/(T_{hi} - T_{ci}) \quad (22)$$

Considering overall heat transfer coefficient, the heat exchanger surface area (A) is computed by,

$$A = \frac{Q}{UFLMTD} \quad (23)$$

For sensible heat transfer, the heat transfer rate is given by, $Q = m_h C_{ph}(T_{hi} - T_{ho}) = m_c C_{pc}(T_{co} - T_{ci})$ (24)

Based on total heat exchanger surface area (A), the necessary tube length (L) is, $L = \frac{A}{\pi d_o N_t}$ (25)

$$\Delta P_t = \Delta P_{\text{tube length}} + \Delta P_{\text{tube elbow}} \quad (26)$$

$$\Delta P_t = \frac{\rho_t v_t^2}{2}\left(\frac{L}{d_i} f_t + p\right) n \quad (27)$$

Different values of constant p are considered by different authors. Kern assumed p = 4, whileSinnot et al. assumed p = 2.5. The shell side pressure drop is,

$$\Delta P_s = f_s \left(\frac{\rho_s v_s^2}{2}\right)\left(\frac{L}{B}\right)\left(\frac{D_s}{d_e}\right) \quad (28)$$

Where, $f_s = 2 b_o Re_s^{-0.15}$ (29)

And $b_o = 0.72$, valid for $Re_s < 40{,}000$.

Considering pumping efficiency (η), pumping power computed by,

$$P = \frac{1}{\eta}\left(\frac{m_t}{\sigma_t}\Delta P_t + \frac{m_s}{\sigma_s}\Delta P_s\right) \quad (30)$$

The objective function has been assumed as the total present cost

$$C_{tot} = C_i + C_{oD} \quad (31)$$

The capital investment C_i is computed as a function of the exchanger surface adopting Hall's correlation

$$C_i = a_1 + a_2 S^{a3} \quad (32)$$

Where $a_1 = 8000$, $a_2 = 259.2$ and $a_3 = 0.91$ for exchangers made with stainless steel for both shells and tubes.

The total discounted operating cost related to pumping power to overcome friction losses is instead computed from the following equations:

$$C_{oD} = \sum_{k=1}^{ny} \frac{C_o}{(1+i)^k}, \quad (33)$$

$$C_o = P . C_E . H \quad (34)$$

4. Implementation of Algorithm

"gamultiobj" finds a local Pareto front for multiple objective functions using the genetic algorithm. For this example, we will use "gamultiobj" to obtain a Pareto front for two objective functions described in the MATLAB file. It is a real-valued function on that consists of two objectives, each of three decision variables. We also impose bound constraints on the decision variables

The default initial population is created using a uniform random number generator. Default values for the population size and the range of the initial population are used to create the initial population. The default population size used by "gamultiobj" is '15*numberOfVariables'. The initial population is generated using a uniform random number generator in a default range of [0; 1]. This creates an initial population where all the points are in the range 0 to 1.

The adopted ''Crossover Fraction'' parameter, i.e. the percentage of individuals of each generation, excluding the Elite Count individuals, which are generated through a crossover recombination of selected individuals of the previous generation was 0.8. The selection algorithm used for picking the parent individuals was the tournament in which parents are picked with a probability proportional to

their fitness function. The crossover method utilized is the so-called crossover-scattered, where a random binary vector is created having a number of bits equal to the number of genes of an individual. Then, the genes where the value is 1 are copied from the first parent, while the genes where the value is 0 are copied from the second parent. The obtained genes are then combined to form the child.

The number of best performing individuals of a generation which are transferred to the next one (Elite count) was set at 2. The percentage of individuals who undergo a mutation derives instead from the previously defined parameters in that all individuals who are not bred and are not part of the elite count are subject to mutation. Finally, migration of individuals from previous generations is allowed each twentieth third generation. The number of transferred individuals is ((PopulationSize -EliteCount) * MigrationFraction) where the migration fraction was set at 0.2. Those migrant individuals substitute the worst individuals of the current generation.
We choose the default distance measure function, @distancecrowding, which is provided in the toolbox to calculate the distance measure of an individual. The crowding distance measure function in the toolbox takes an optional argument to calculate distance either in function space (phenotype) or design space (genotype). If 'genotype' is chosen, then the diversity on a Pareto front is based on the design space. The default choice is 'phenotype' and, in that case, the diversity is based on the function space. Here we choose 'genotype' for our distance function. We will pass our options structure 'options', created above, to "gaoptimset" to modify the value of the parameter 'DistanceMeasureFcn'. We select the default value 0.35 of the Pareto fraction i.e., the solver will try to limit the number of individuals in the current population that are on the Pareto front to 35% of the population size.
"gamultiobj" uses three different criteria to determine when to stop the solver. The solver stops when any one of the stopping criteria is met. It stops when the maximum number of generations is reached; by default this number is 1000. However, in the tests convergence was always obtained within about 500 generations. "gamultiobj" also stops if the average change in the spread of the Pareto front over the 'StallGenLimit' generations (default is 100) is less than tolerance(Default value: 1e-4) specified in options, TolFun. The third criterion is the maximum time limit in seconds (default is Infinite).

We do not use any hybrid functionality scheme to arrive at the optimal pareto front. The gamultiobj solver is run, the solutions found on the Pareto front are displayed and the average distance measure of solutions is calculated. A smaller average distance measure indicates that the solutions on the Pareto front are evenly distributed. However, if the Pareto front is disconnected, then the distance measure will not indicate the true spread of solutions. The Pareto Front and Average Pareto Spread are plotted with an interval of 1 generation.

A total of 4 design variations are considered for the optimization**.**
Case 1: n= 2, Square tube layout
Case 2: n = 2, Triangular tube layout
Case 3: n = 4, Square tube layout
Case 4: n = 4, Triangular tube layout

The three design variables are:-
1. Tube outside diameter (d_0)
2. Shell inside diameter (D_s)
3. Baffle spacing (B)

Two objective functions are simultaneously optimized to obtain a set of solutions that yield the best values for both functions
1. The cost which consists of the initial investment and the annual cost of operation
2. Length of the heat exchanger

The optimization toolbox in MATLAB is used for implementation of multi-objective optimization using Genetic Algorithm. The solver used is "gamultobj" and the settings are fixed as following:-
Population Type: Double Vector
Creation Function: Constraint Dependent
Population Size: Default (15*No of variables)
Initial Population: Default
Initial Scores: Default
Selection Function: Tournament
Tournament size: Default (2)
Crossover Fraction: Default (0.8)
Mutation Function: Constraint Dependent
Crossover Function: Intermediate
Crossover Ratio: Default (1)
Migration Direction: Forward
Migration Fraction: Default (0.2)
Migration Interval: Default (20)
Distance Measure Function: Default @distancecrowding
Pareto Front Population Fraction: Default (0.35)
Hybrid Function: fgoalattain
Maximum Generations: 1000
Time Limit: Default (Infinite)
Fitness Limit: Default (Infinite)
Stall Generations: Default (100)
Function Tolerance: 1e-4

Empirical and Statistical data

The shell side fluid and tube side fluids are distilled water and raw water respectively.
$C_{ph} = C_{pt} = C_{ps} = 4.18$ KJ/Kg K
$R_{foul,shell} = R_{foul,tube} = 0.00017 m^2K/W$
$\rho_t = 999$ kg/m^3
$\rho_s = 995$ k/m^3
$\mu_s = 0.008$ pa s
$\mu_t = 0.00092$ pa s
$T_{ci} = 23.9^0$C
$T_{co} = 26.7^0$C
$T_{hi} = 33.9^0$C
$T_{ho} = 29.4^0$C
$K_t = 0.62$ W/mK
$K_s = 0.62$ W/mK
$m_h = m_s = 22.07$ kg/s
$m_t = 35.31$ kg/s

$b_0 = 0.72$
$d_i = 0.8\ d_0$
$Pt = 1.25\ d_0$
ny = 10 years
i = 10%
C_e= 0.12 units/KWh
H = 7000 yr/hr

The values of the constants C and n_1 are taken as follows

Table1: The table of C and n_1 constant values

	Case 1	Case 2	Case 3	Case 4
C	0.156	0.249	0.158	0.175
n_1	2.291	2.207	2.263	2.285

Assumptions:
$Re_t > 10000$
$Re_s < 40000$
Kern assumption (p=4)

Variable Bounds:
$0.015 \leq d_0 \leq 0.051$
$0.05 \leq B \leq 0.5$
$0.1 \leq D_s \leq 1.5$

4. Results and Discussion

4.1 Case 1

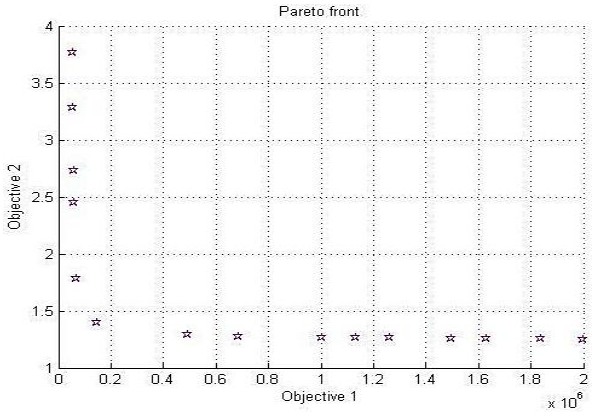

Figure 2: Pareto front depicting the optimal points for Case 1

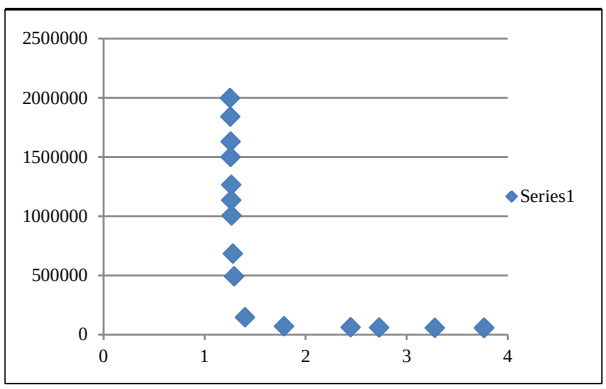

Figure 3: The variation of cost function with length of the heat exchanger for Case 1

Table 2: The table of optimal points and corresponding functional values for Case 1:

	f(1)	f(2)	X1	X2	X3
1	1995992	1.253852	0.015005	0.050006	1.49999996
2	53242.4	3.767434	0.015005	0.499994	0.75569973
3	1626856	1.258168	0.015005	0.053912	1.49999996
4	682542.7	1.280339	0.015006	0.074948	1.49893103
5	1497419	1.260781	0.015005	0.055601	1.49911993
6	1838280	1.256146	0.015008	0.051543	1.49967581
7	53242.4	3.767434	0.015005	0.499994	0.75569973
8	1003543	1.270012	0.015007	0.064594	1.49944063
9	143647.8	1.400892	0.01502	0.157123	1.44308041
10	66804.41	1.787831	0.015005	0.438604	1.28007336
11	489623.6	1.292702	0.015008	0.085657	1.49624822
12	59118.51	2.449016	0.015007	0.423265	0.9976701
13	55659.61	2.729828	0.015009	0.495414	0.93928776
14	1132994	1.266791	0.015005	0.061698	1.49950647
15	1261123	1.264304	0.015006	0.059266	1.49967055
16	54120.71	3.281879	0.015007	0.485797	0.82514739

In the first case we observe that the minimum of f(1)(=53242.4) is obtained at the point (d_0=0.015005, B=0.49999, D_s=0.7557). But that point also has the maximum value for length (=3.7674) among all optimal points. Analogously the least value of f(2) of 1.2538 is at the point (d_0=0.15005, B=0.050005, D_s=1.5), but with the maximum value(=1992995) of the cost function in the list of optimal points. Also it can be noted that for all the optimal points the value of d_0 is close to 0.015. The list of all feasible solutions with their functional values, the pareto front and the variation of cost function with length of the heat exchanger have been illustrated in (Table 2), (Figure 2) and (Figure 3), respectively.

4.2 Case 2

Table 3: The table of optimal points and corresponding functional values for Case 2

	f(1)	f(2)	X1	X2	X3
1	50203.7	7.750892	0.01661	0.487396	0.530987
2	174555.3	2.535273	0.016133	0.099044	1.498579
3	253185.9	2.522927	0.016133	0.074852	1.498398
4	302366.2	2.518645	0.016133	0.067478	1.498587
5	55813.66	5.817907	0.016574	0.373452	0.65661
6	58633.08	4.88362	0.016274	0.411127	0.756528
7	423595.5	2.512074	0.016132	0.056833	1.498633
8	226041.5	2.525847	0.016133	0.080585	1.498575
9	391206.8	2.513735	0.016134	0.059053	1.49857
10	126586.7	2.562349	0.016133	0.161544	1.498579
11	51471.08	6.901998	0.016423	0.444906	0.571023
12	50203.7	7.750892	0.01661	0.487396	0.530987
13	61680.07	4.57523	0.016362	0.39078	0.80761
14	54451	5.87219	0.016218	0.39287	0.638104
15	347773.9	2.515787	0.016133	0.062638	1.498588
16	423595.5	2.512074	0.016132	0.056833	1.498633

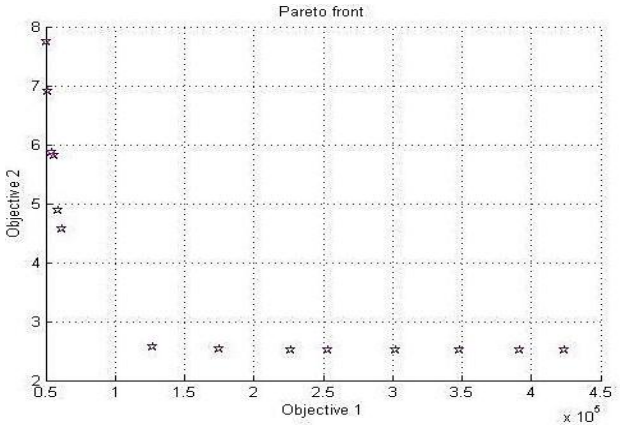

Figure 4: Pareto front depicting the optimal points for Case 2

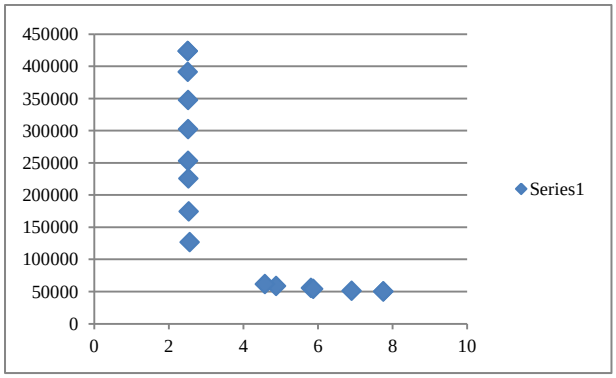

Figure 5: The variation of cost function with length of the heat exchanger for Case 2

In the second case we notice a similar trend. The minima for the first objective function occurs at (d_0=0.01661, B=0.487396, D_s=0.530987) with a cost value of 50203.7, but at the same time with largest length (=7.750892) among all optimal points. On the other hand, at (d_0=0.016132, B=0.056833, D_s=1.498633), we obtain the minimum possible length (=2.512074) but also the largest cost value (=423595.5) among the points. Analogous to case 1, all the optimal points had the values of outer tube diameter close to 0.016. The list of all feasible solutions with their functional values, the pareto front and the variation of cost function with length of the heat exchanger have been illustrated in (Table 3), (Figure 4) and (Figure 5), respectively.

4.3 Case 3

Table 4: The table of optimal points and corresponding functional values for Case 3

	f(1)	f(2)	X1	X2	X3
1	1382230	416.4354	0.05099985	0.5	0.948281
2	2.08E+08	241.9545	0.01500109	0.052165	1.499999
3	7.44E+07	241.9939	0.01500384	0.076317	1.49999
4	1.63E+07	244.8743	0.01566322	0.145053	1.498017
5	1382230	416.4354	0.05099985	0.5	0.948281
6	1.24E+08	241.9692	0.01500139	0.063086	1.499992
7	3146567	331.8706	0.05007102	0.217882	1.491477
8	5393604	288.0674	0.02911973	0.208352	1.489072
9	1.78E+08	241.959	0.0150012	0.055233	1.499996
10	1.95E+08	241.9562	0.01500109	0.053439	1.499999
11	1.04E+08	241.9732	0.0150013	0.067203	1.499996
12	3975894	300.0257	0.02053496	0.363654	1.122275
13	6431416	251.141	0.01608984	0.319452	1.440522
14	5.24E+07	242.0047	0.01500328	0.087425	1.499964
15	1755124	359.6938	0.04980531	0.442119	1.262807
16	1383275	413.1487	0.05099986	0.499999	0.963652

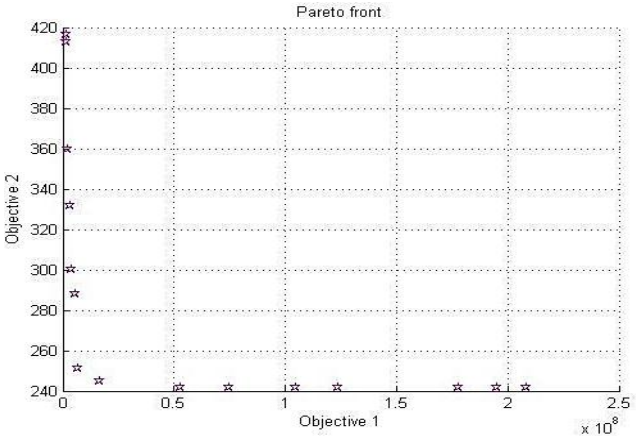

Figure 6: Pareto front depicting the optimal points for Case 3

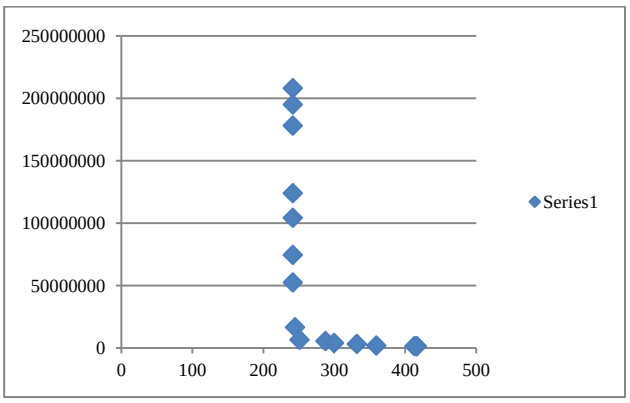

Figure 7: The variation of cost function with length of the heat exchanger for Case 3

In the third case we observe that the minimum of f(1) (= 1382230) is obtained at the point (d_0=0.051, B=0. 5, D_s=0.948281). But that point also has the maximum value for length (=416.4354) among all optimal points. Analogously the least value of f(2) of 241.9545is at the point (d0=0.015001, B=0.052165, D_s=1.499999), but with the maximum value(=2.08E+08) of the cost function in the list of optimal points. The list of all feasible solutions with their functional values, the pareto front and the variation of cost function with length of the heat exchanger have been illustrated in (Table 4), (Figure 6) and (Figure 7), respectively.

4.4 Case 4

In the fourth case we observe that the minimum of f(1)(= 66155.38) is obtained at the point (d_0=0.049461,

B=0.49999, D_s=1.499961). But that point also has the maximum value for length (=7.775957) among all optimal points. Analogously the least value off(2) of 1.449332is at the point (d_0=0.015005, B=0.052773, D_s=1.499951), but with the maximum value(=1.28E+07) of the cost function in the list of optimal points. The list of all feasible solutions with their functional values, the pareto front and the variation of cost function with length of the heat exchanger have been illustrated in (Table 5), (Figure 8) and (Figure 9), respectively.

Table 5: The table of optimal points and corresponding functional values for Case 4

	f(1)	f(2)	X1	X2	X3
1	66155.38	7.775957	0.049461	0.49999	1.499961
2	66155.38	7.775957	0.049461	0.49999	1.499961
3	1.28E+07	1.449332	0.015005	0.052773	1.499951
4	1765662	1.527018	0.015415	0.105802	1.49979
5	1.28E+07	1.449332	0.015005	0.052773	1.499951
6	69219.47	2.829932	0.023279	0.497548	1.499825
7	3115350	1.467734	0.015013	0.087028	1.49981
8	66324.57	6.098001	0.041308	0.499978	1.499843
9	9175549	1.453202	0.015005	0.059365	1.49972
10	465306	1.571534	0.015555	0.17355	1.499823
11	69090.95	4.231669	0.031607	0.466695	1.499853
12	4799939	1.461389	0.015009	0.07464	1.499806
13	7701611	1.455654	0.015009	0.063145	1.499722
14	1.02E+07	1.451919	0.015005	0.05719	1.499824
15	66195.73	7.030898	0.045909	0.499808	1.499911
16	71460.67	2.043988	0.018211	0.49999	1.499961

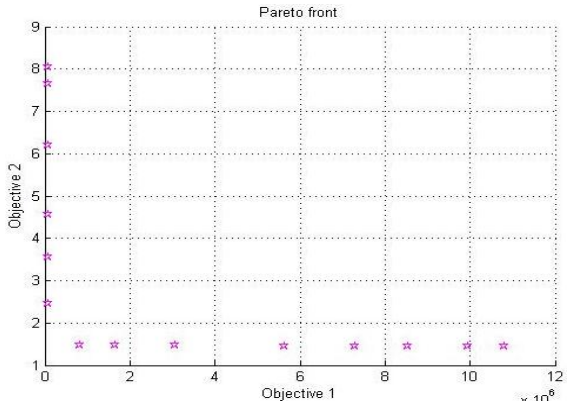

Figure 8: Pareto front depicting the optimal points for Case 4

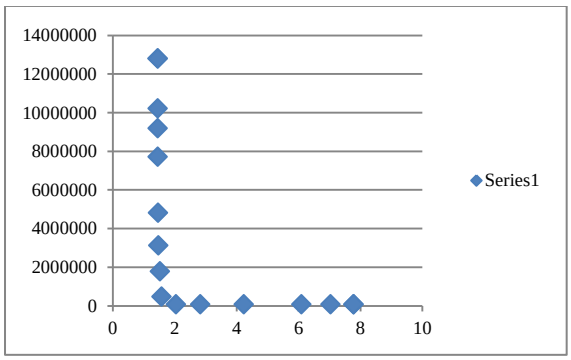

Figure 9: The variation of cost function with length of the heat exchanger for Case 4

Table 6: Comparison of present work with caputo*et al* (2008) and literature

	Literature	Caputo et al	Present Work
D_s	0.387	0.620	0.530987
d_0	0.019	0.016	0.01661
B	0.305	0.440	0.487396
Annual Capital Cost	43,989	20,834	50203.7
Length	4.880	1.548	7.750892

In Table 6, the values of the design variables and heat exchanger length corresponding to the minimum annual expenditure obtained in the present work has been compared to those in literature and the results of caputo *et al*(2008),. The slight dissimilarity with the findings of caputo et al could be attributed to the fact that the values of number of tube passes (n) and tube layout structures considered for calculation are different in both cases. The tubeside and shellside Reynold's numbers (R_t and R_s) have been assumed to be in different ranges. Also different values have been assumed for the constant 'p', which is used for computing the tubeside pressure drop.

5. Conclusion

Annual cost and length of heat exchanger are opposing entities; i.e. increase in one, invariable produces reduction in the other. This could be attributed to the fact that the daily operating cost is inversely proportional to average duration of operation per day. When the length of the heat exchanger increases, so does the net surface area available for heat exchange, due to which the overall efficiency of heat transfer for a heat exchanger of a given duty cycle and given temperature difference between working fluids increases. Hence it needs to work for ewer hours.

When the number of tube passes is two, the obtain overall lower values of the cost function in case of the square pitch than in case of triangular and conversely, lower values of length in case of the triangular pitch than in case of square . On the other hand, when the number of tube passes is four we obtain overall lower values for both cost and length functions in case of the triangular pitch than in case of the square pitch.

When the number of tube passes is increased from two to four there is a substantial rise in the cost function values for the square layout a moderate increase in case of the triangular layout. This could be attributed to the fact that an increase in the overall values of the tube outer diameter (as indicated in the tables 1 2, 3 and 4), results in a decrease in the area of flow available on the shellside and hence an increase in the shellside flow velocity. This phenomenon causes a considerably higher shell side pressure drop and a marked rise in the shellside annual pumping cost. This is in contrast with the tubeside conditions as the number of tube passes results in decrease in the tube side flow velocity, for a given tubeside mass flow rate. This leads to a decrease in the tubeside pressure drop and hence a lower value of the annual tubeside pumping cost. But the increase in the shellside pumping

cost supersedes decrease in the tubeside pumping cost. This causes a net increase in the total annual cost.

On the other hand, when the number of tubes is increased, there is a tremendous rise in the overall length values for the square layout. Increase in shellside flow velocity leads to higher shellside heat transfer coefficient and analogously, decrease in the tubeside low velocity causes lower tubeside heat transfer coefficient. This results in a lower overall heat transfer coefficient of the heat exchanger. Hence the surface area, and equivalently length the heat exchanger required for a given duty, increases. But we also note a marked decrease for length in case of the triangular pitch. This is because in this case there is a net rise in the overall heat transfer coefficient.

It can be seen that when the number of tubes is two, dimensions close to [d_0=0.015, B=0.5] favour lower cost function values. On the contrary, when dimensions are close to [B=0.05, D_s=1.5], we tend to get lesser length values. It can be seen that when the number of tubes is two, dimensions close to [d_0=0.05, B=0.5] favour lower cost function values. On the contrary, when dimensions are close to [d_0=0.015, B=0.05, D_s=1.5], we tend to get lesser length values.

Thus, in general for lower annual cost values we need the baffle spacing to be approximately 0.5. But for smaller lengths we want baffle space and inner shell diameter to be close to 0.05 and 1.5 respectively. We get highest values of both cost function and length for square tube layout and 4 tube passes among all the four cases.

References

J.E. Mott, J.T. Pearson, and W.R. Brock (1972), Computerized design of a minimum cost heat exchanger, *ASME Paper 72-HT-26*

K.R. Ramananda, U. Shrinivasa, and J. Srinivasan (1991), Synthesis of cost-optimal shell-and-tube heat exchangers, *Heat Transfer Engineering*, vol.. 12, pp. 47–55

M. Kovarik (1989), Optimal heat exchangers, *Journal of Heat transfer*, vol. 111, pp. 287–293

M. Saffar-Avval, and E. Damangir (1995), A general correlation for determining optimum baffle spacing for all types of shell and tube exchangers, *International Journal of Heat and Mass Transfer*, vol. 38, pp. 2501–2506

S.K. Jenssen (1969), Heat exchanger optimization, *Chemical Engineering Progress*, vol. 65, pp. 59–65

D.H. Fax, and R.R. Mills (1957), Generalized optimal heat exchanger design, *ASME Transactions*, vol. 79, pp. 653–661

A. Unuvar, and S. Kargici (2004), An approach for optimum design of heat exchangers, *International Journal of Energy Research*, vol. 28, pp. 1379–1392

H.J. Fontein, and J.G. Wassink (1978), The economically optimal design of heat exchangers, *Engineering and Process Economic*, pp. 141–149

J.W. Palen, T.P. Cham, J. Taborek (1974), Optimization of shell-and-tube heat exchangers by case study method, *Chemical Engineering Progress Symposium Series*, vol. 70, pp. 205–214

H. Paul (1982), An application of geometric programming to heat exchanger design, *Computers and Industrial Engineering*, vol. 6, pp. 103–11.

P.D. Chauduri, U. Diwekar, and J. Logsdon (1997), An automated approach for the optimal design of heat exchangers, *Industrial Engineering Chemical research*, vol. 36, pp. 3685–36.

R. Selbas, O. Kizilkan, and M. Reppich (2006), A new design approach for shell-and-tube heat exchangers using genetic algorithms from economic point of view, *Chemical Engineering and Processing*, vol. 45, pp. 268–275

A.C. Caputo, P.M. Pelagagge, and P. Salini (2008), Heat exchanger design based on economic optimization, *Applied Thermal Engineering*, vol. 28,pp. 1151–1159

Nomenclature

C_{ps}→ Shell side specific heat
C_{pt} →Tube side specific heat
$R_{foul,shell}$ → Shell side fouling resistance
$R_{foul,tube}$ → Shell side fouling resistance
ρ_t→ Tube side Fluid Density
ρ_s →Shell side Fluid Density
μ_s→Viscosity at shell wall
μ_t→Viscosity at tubewall
T_{ci} → Cold fluid inlet temperature
T_{co}→Cold fluid outlet temperature
T_{hi} →Hot fluid inlet temperature
T_{ho}→Hot fluid outlet temperature
k_t→ Tube side conductive heat transfer coefficient
k_s→ Tube side conductive heat transfer coefficient
m_s→ Shell side mass flow rate
m_t→Tubeside mass flow rate
b_0 ,C, n_1, p→ Numerical constants
d_i→ Inner Tube diameter
Pt→ Tube Pitch
ny→Equipment life
i→ Interest rate
Ce→Energy Cost
H →Annual operating time
n→ Number of tube passes
Re_s→Shell side Reynolds Number
Re_t→ Tube side mass flow rate
Pr_s→Shell side Prandtl Number
Pr_t→Shell side Prandtl Number
h_s→ Shell side convective heat transfer coefficient
h_t→ Tube side convective heat transfer coefficient
U→Overall heat transfer coefficient
F→ Temperature Difference corrective factor
P→ Pumping power
Q→Heat Duty
L→ Length of heat exchanger
S→Surface area of heat exchanger
ΔT_{ML} →Logarithmic mean temperature difference
ΔP_s→Shell side pressure drop
ΔP_t→ Tube side pressure drop
Cl→ Clearance
C_{OD}→Annual Operating Cost
C_i→ Initial Investment
C_{tot}→ Total annual cost
N_t→ Number of tubes
f_t→ Darcy tube side friction actor
f_s→ hell side friction factor
η→ Pump efficiency
v_s→ Shell side flow velocity
v_t→ Tube side flow velocity
d_e→ Equivalent shell diameter